

# Design of Reconfigurable Supernumerary Robotic Limb Based on Differential Actuated Joints

Qinghua Zhang, Yanhe Zhu, Xiang Zhao, Yeqin Yang, Hongwei Jing, Guoan Zhang, Jie Zhao

**Abstract**—This paper presents a wearable reconfigurable supernumerary robotic limb with differential actuated joints, which is lightweight, compact and comfortable for the wearers. Compared to the existing supernumerary robotic limbs which mostly adopted series structure with large movement space but poor carrying capacity, a prototype with the series-parallel configuration to better adapt to different task requirements has been developed in this design. To achieve a compact structure, two kinds of cable-driven mechanical structures based on guide pulleys and differential actuated joints were designed. Moreover, two different tension devices were also designed to ensure the reliability and accuracy of the cable-driven transmission. The proposed device also employed self-designed bearings which greatly simplified the structure and reduced the cost.

**Keywords**—Cable-driven, differential actuated joints, reconfigurable, supernumerary robotic limb.

## I. INTRODUCTION

**I**N the industrial fields, such as nuclear industry maintenance and large aircraft manufacturing, the following challenges exist: 1) Restricted work posture. 2) Complex assembly process. 3) Long-term work fatigue. 4) Increasing the aging of the workforce. These challenges greatly reduce the efficiency of industrial production. Although many industrial robots have been put into use in these industrial fields, the base of most industrial robots cannot be flexibly adjusted according to the needs of workers. Exoskeleton robots have been used for power augmentation which were attached to the body and greatly increased the strength of the human limbs [1]. However, it is difficult to perform the complex assembly process which requires assistance from others. The concept of supernumerary robotic limb (SRL) was first proposed by MIT's Asada team [2], [3]. Compared with the industrial robot, the SRL can move with the wearer and adjust the task requirements according to the intention of the wearer. Unlike the exoskeleton, the SRL is an extra arm or finger, which is independent of the human body and can work with the human [4]. Wearable robots can play an important auxiliary role in the above operation occasions.

Many researchers have developed different types of wearable SRL with auxiliary functions [5]-[13]. Praticchizzo et al. [5] proposed a modular extra-finger which is opposite to the

palm to improve the grasping ability of human hand. Wu et al. [6]-[8] have developed three kinds of similar mechanical structures with two mechanical fingers worn on the wrist, which could help the wearer to achieve the task of unscrewing the cap. A kind of soft-sixth finger was driven by a string, which could help patients achieve grasping function with upper limb hemiplegia [9]. However, these supernumerary fingers are not suitable for the application of the above mentioned industrial fields due to the only small areas of cooperation with both hands and limited output capacity. Llorens et al. [10] developed a five degree of freedoms (DOF) wearable robot on the shoulder directly driven by DC motors. Parietti et al. [4], [11] designed two kinds of similar supernumerary limbs actuated by a brushless DC motor through a harmonic drive gearbox. Their elbow actuators were both placed behind the shoulder to decrease the inertia of SRL. The actuation unit transmits the power through belt driving system or cable driving system. Due to the other joints are still driven in traditional ways, the overall equipment still appears to be less lightweight. Vatsal et al. [12] proposed a five DOF wearable robotic forearm with light weight for close-range human-robot collaboration. However, it sacrifices the size and range of motion (ROM) of the device. Nguyen et al. [13] developed a soft poly-limb but this mechanism has limited strength. Most of the existing SRL systems have serial structures with the characteristics of large movement space, high flexibility and simple control. However, the carrying capacity of the serial mechanism is worse compared to the parallel mechanism.

To address these limitations, a compact and reconfigurable SRL based on differential actuated joints is designed in this paper. It aims at helping the wearer work more efficiently with the functions of auxiliary support, load operation and delicate operation. Compared with the existing SRL, the main advantages of the SRL presented in this paper can be summarized as: 1) adopting the series-parallel configuration design, two 3-DOF series limbs can be combined into a 5-DOF parallel limb with the characteristics of large movement space and high stiffness; 2) the driving of shoulder and elbow flexion/extension joint adopt the method of differential actuated joints, which make the load for each DOF can be shared by two motors at the same time. This type of driving not only greatly shares the burden of the motor but also increases the compactness of structure; 3) all transmission ways adopt the cable-driven transmission based on the guide wheel structure, which makes the mechanical device extremely lightweight and compact; 4) the newly designed wire rope pre-tightening mechanism greatly improves the reliability and accuracy of cable-driven transmission and the bearings used in this article greatly

Qinghua Zhang, Xiang Zhao, Yeqin Yang, Hongwei Jing, Jie Zhao are with Harbin Institute of Technology University, Heilongjiang Province 150006, China (e-mail: m13349395254@163.com, zxhit2018@163.com, youngyeqin@163.com, jhw\_hit@163.com, jzhao@hit.edu.cn).

Guoan Zhang is with TaiZhou University, Zhejiang Province 317700, China. (e-mail: zga0523@126.com).

Yanhe Zhu is with Harbin Institute of Technology University, Heilongjiang Province 150006, China (corresponding author, phone: 13074594165; fax: +86-045186414538, e-mail: yhzhu@hit.edu.cn).

simplified the structure and reduced the cost.

## II. MECHANICAL DESIGN

### A. The Distribution of DOF and Configuration Design

After simplification, the human upper limb can generally be composed of 7 DOF including shoulder flexion/extension, shoulder abduction/adduction, shoulder internal/external rotation, elbow flexion/extension, forearm supination/pronation, wrist flexion/extension and wrist radial deviation/ulnar deviation. As an extension of the human limb, SRL should have similar DOF layout and dynamic characteristics compared with the human upper limb. The reasons are as follows: 1) it is unallowed to interfere with people during the assisted operation; 2) It is easier for the wearer to think that it is

part of his body during the assisted operation of SRL [2], [3]. To develop an inherently safe SRL without influencing performance, the following design factors should be required: 1) Low mass and high precision, 2) high output characteristic, 3) sufficient DOF without losing the aforementioned requirements. Taking full account of these design factors, the whole SRL used the cable-driven transmission with high accuracy, smooth transmission and low mass compared with other traditional ways of transmission. The series-parallel configuration design enables the SRL to have the characteristics of high flexibility, large movement space and strong carrying capacity compared with the traditional configuration.

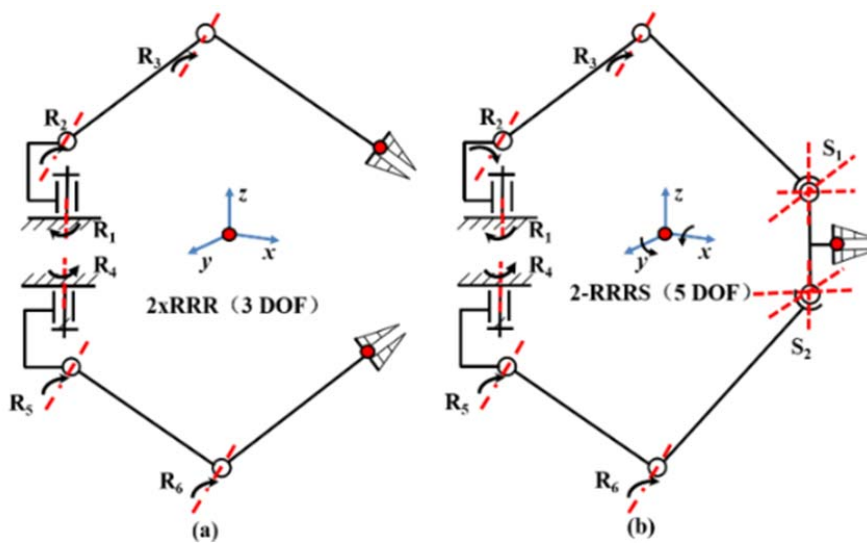


Fig.1 (a) DOF layout of the series configuration, (b) DOF layout of the parallel configuration

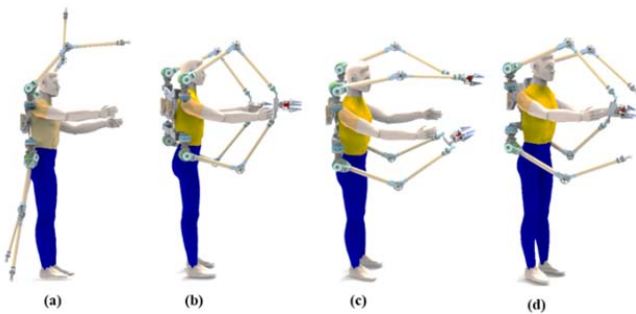


Fig. 2 (a) The configuration of series mode, (b) parallel configuration 1, the parallel mode is formed by the vertical combination, (c) parallel configuration 2, the parallel mode is formed by the horizontal combination, (d) parallel configuration 3, the parallel mode is formed by the cross combination

The distribution of DOF is shown in Fig. 1 and Fig. 2 shows the variable configurations of SRL worn in the human model. In series mode, the whole model consists of four limbs, each of which has three DOF. In the working scene with limited posture, it has functions of auxiliary support and unloading. In parallel mode, the whole model consists of two limbs, each of

which has five DOF with functions of load operation and delicate operation. For all combinations of parallel configurations, the end-effector could realize the orientation transformation of yaw, pitch and roll, which indirectly make the limb reach up to 6 DOF indirectly. In nuclear maintenance and large aircraft manufacturing processes, it also can quickly switch different configurations in the face of different working scenes to better adapt to different task requirements.

### B. The Overview of the SRL

As previously mentioned, the characteristics of high precision, large movement space, high stiffness and low mass are crucial for SRL. Furthermore, a proper combination of the proposed mechanisms, having similar or higher dynamic characteristics compared with the human upper limb is also valuable. Taking all these factors into consideration, we propose a variable configuration mechanism of SRL based on the cable-driven transmission with high accuracy, smooth transmission and low mass [14]. Fig. 3 (a) shows the 3 DOF of series SRL model and Fig. 3 (b) shows the 5 DOF of the parallel SRL model. The upper and lower limbs have a size of 350 and 330 mm, respectively. To reduce the rotational inertia, motors

for the elbow are placed at the proximal end. Considering the torque on the shoulder abduction/adduction direction is much smaller than the other two motion directions, we set the transmission ratio as 1:4 and 1:6 respectively. The models of

shoulder abduction/adduction part, differential actuated joints part and series-parallel conversion interface part are shown in Figs. 3 (c)-(e), respectively.

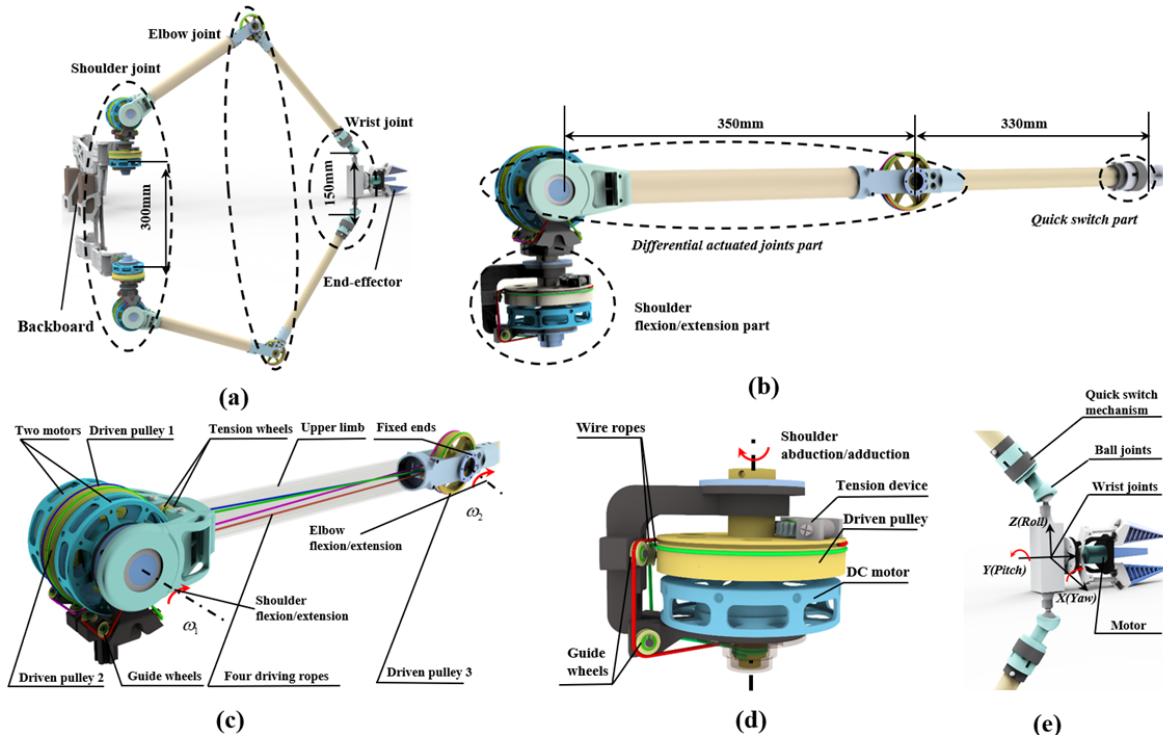


Fig. 3 (a) The 3 DOF of series SRL model, (b) the 5 DOF of parallel SRL model, (c) the model of the shoulder abduction/adduction part, (d) the model of the differential actuated joints part, (e) the model of conversion interface part

### C. The Shoulder Abduction/Adduction Part

Considering the kinematical characteristics of the shoulder abduction/adduction motion, a different mechanism illustrated in Fig. 4 (a) is established and the schematic diagram of this part is shown in Fig. 4 (b). Due to the one-way transmission of the flexible body, two cables are needed for each DOF of the cable-driven limb. In Fig. 4 (a), the red and green lines represent a pair of wire ropes controlling the forward and reverse rotation of driven pulley respectively, and the wire ropes start with the motor output axis and ends with the worm gear and worm pre-tightening device. The traditional cable driving mechanism principle for single joint is shown in in Figs. 4 (c) and (d). In Figs. 4 (c) and (d), the radiuses of the driving pulley and driven pulley are  $R_a$  and  $R_b$ , respectively. It is clear that the transmission ratio  $i = R_a/R_b$ . The pitch of driving pulley is  $p_1$ , the pitch of driven pulley  $p_2$  is simply:

$$p_2 = ip_1, \quad (1)$$

The axial transmission distance of driving pulley and driven pulley which is shown in Fig. 4 (c) can be expressed as:

$$x_1 = ip_1, \quad (2)$$

$$p_2 = x_2, \quad (3)$$

where,  $x_1$  is the axial transmission distance of driving pulley and  $x_2$  represents the axial transmission distance of driven pulley. Combining with (1)-(3), we can get  $x_2 = x_1$ . Inspired by the traditional cable driving mechanism for single joint, the use of guide pulleys greatly increases the compactness of the structure without affecting the function. The specific performances are as follows: 1) In Fig. 4 (b), we could easily get  $x_2 \approx 2x_1/i$ , which greatly reduces the axial transmission distance of driven pulley. 2) Compared with the traditional system, the input and output axes are on the same axis in the improved transmission system, which greatly reduces the radial space distance.

Considering that the large rolling bearings take up more space, we employed a similar structure which places balls in a trench as a simplified rolling bearing. The balls reduce the cost and greatly increase the compactness of the structure [15].

### D. The Differential Actuated Joints Part

Shoulder and elbow flexion/extension are two important DOF which determine the maximum terminal load in the vertical direction. The approach of differential actuated joints applies to the two DOF which effectively shares the burden of the motor and increases the compactness of structure. The

model of this part is shown in Fig. 5 (a) and the schematic diagram of the differential actuated joints is shown in Fig. 5 (b).

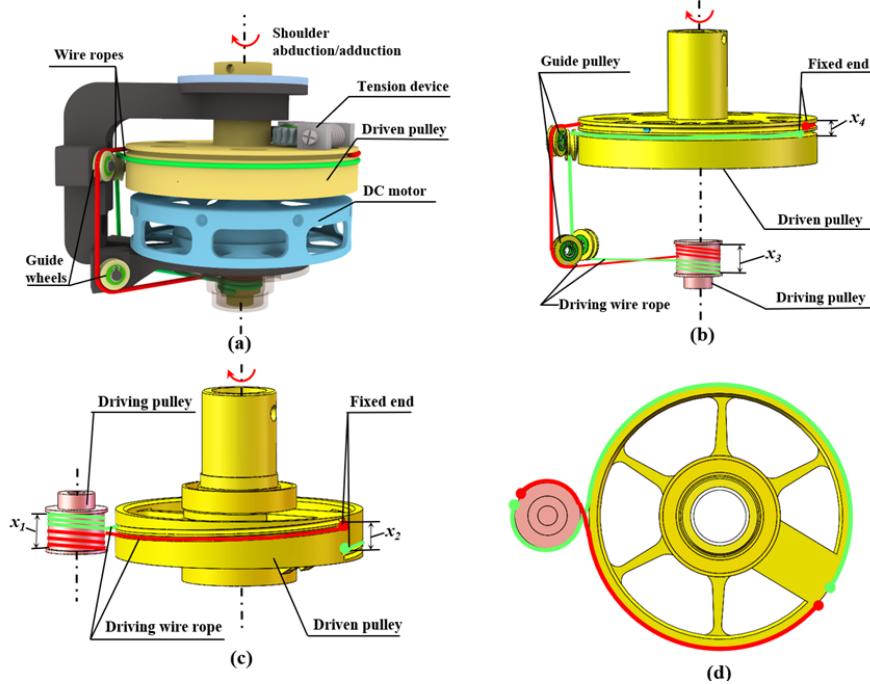


Fig. 4 (a) The model of the shoulder abduction/adduction part, (b) the schematic diagram the shoulder abduction/adduction part, (c) traditional cable driving mechanism principle of axonometric drawing (d) traditional cable driving mechanism principle of top view

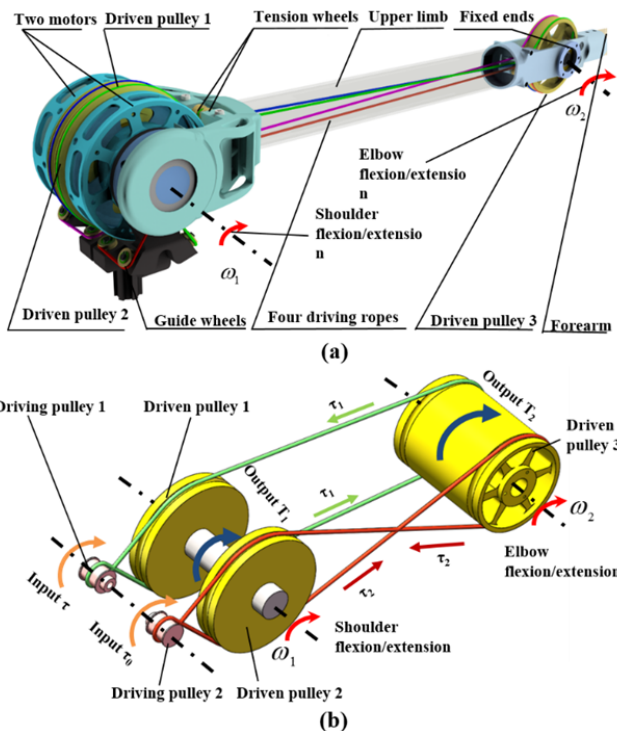


Fig. 5 (a) the model of the differential actuated joints part, (b) the schematic diagram of the differential actuated joints

The driven pulley 1 and the driven pulley 2 can rotate freely around the shoulder flexion/extension axis and the driven

pulley 3 can rotate with the forearm around the elbow flexion/extension axis together. The inputs torque of driving pulley 1 and driving pulley 2 are  $\tau$  and  $\tau_0$ , respectively and the output torque of shoulder flexion/extension and elbow flexion/extension are  $T_1$  and  $T_2$ , respectively. The torque generated by two wire ropes is represented by  $\tau_1$  and  $\tau_2$ , respectively. If the transmission ratio is  $i$ , then  $\tau_1 = i\tau$ ,  $\tau_2 = i\tau_0$ . According to the force analysis of the two driven pulleys, we can get:

$$T_1 = \tau_1 + \tau_2, \quad T_2 = \tau_1 - \tau_2. \quad (4)$$

By simplifying (4), we can get:

$$\tau_1 = \frac{T_1 + T_2}{2}, \quad \tau_2 = \frac{T_1 - T_2}{2}. \quad (5)$$

When the two input wheels rotate in the same direction at the same torque, the following condition holds:

$$\tau_1 = \tau_2. \quad (6)$$

Combining with (4) and (6), we can get:

$$\begin{cases} T_1 = 2\tau_1 \\ T_2 = 0 \end{cases}. \quad (7)$$



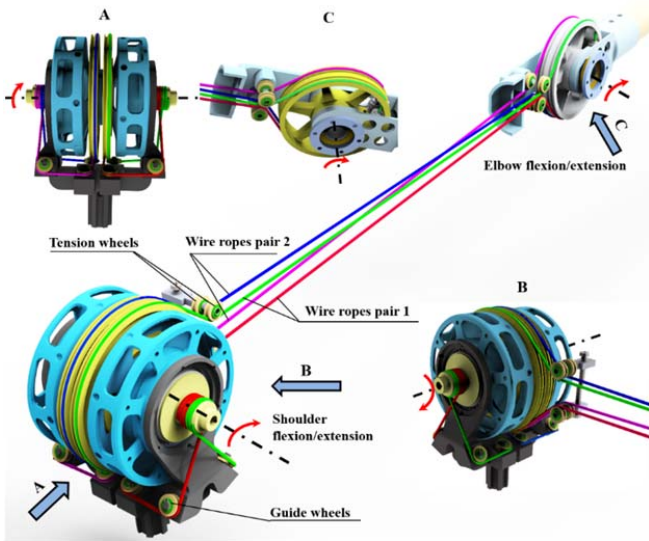


Fig. 6 Detailed wire routing of the differential actuated joints part

This condition generates the motion of shoulder flexion/extension and the torque of the two motors is applied simultaneously to the shoulder joint. When the two input wheels rotate in reverse at the same torque, the following condition holds:

$$\tau_2 = -\tau_1 \quad (8)$$

Combining with (4) and (6), we can get:

$$\begin{cases} T_1 = 0 \\ T_2 = 2\tau_1 \end{cases} \quad (9)$$

This condition generates the motion of elbow flexion/extension and the torque of the two motors is applied simultaneously to the elbow joint. The details of wire routing are shown in Fig. 6. In Fig. 6, the red and green lines represent a pair of wire ropes, and the purple and blue lines represent another pair of wire ropes controlling the forward and reverse rotation of driven pulley respectively.

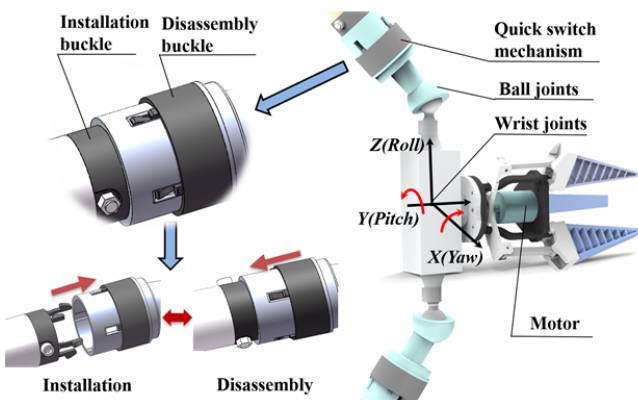


Fig. 7 The model of the conversion interface

### E. The Conversion Interface Part

Considering the convenience and effectiveness of serial-parallel conversion, we use ball joints as the connection interface with an ingenious quick switch device. The model of this part is shown in Fig. 7. The wrist joint motion includes the orientation transformation of yaw and pitch. For all combinations of parallel configurations, the end-effector could realize the orientation transformation of yaw, pitch and roll.

### F. The Pre-Tensioner of the Cable-Driven Mechanism

The pre-tightening and fixing of the wire rope play a vital role in the cable-driven mechanisms and it greatly affects the transmission performance of cable-driven mechanisms. According to different space requirements, two types of effective pre-tightening devices illustrated in Fig. 8 are designed. In shoulder abduction/adduction part, we propose the worm and worm wheel structure to realize the pre-tightening of wire rope due to its self-locking characteristics [16]. In the differential actuated joints part, considering long-distance and large load transmission, we use guide wheel which can be regulated up and down to realize the pre-tightening of wire rope.

The screw can move the guide wheel which can tighten the wire rope in guide wheel pre-tightening part and the force  $F$  provided for pre-tightening on the screw is given as:

$$F = F_2 \times \cos(\theta_1) = (F_1 + F_1) \times \cos(\theta_1) \quad (10)$$

where  $F_2$  is the resultant force of wire rope to the guide wheel,  $F_1$  is the pull on the wire rope and  $\theta_1$  represents the angle between the resultant force and the vertical direction. The locking block and wedge mechanism in fixed end pre-tightening part are used to fix the rope end. In order to ensure timely pre-tightening during the transmission process, we apply one spring to provide the opposite force  $F$ , and the selection of spring stiffness is determined by the tension range of the wire rope. The mechanical equation is given as:

$$F = F_1 = k\Delta_x \quad (11)$$

where  $F_1$  is the pull on the wire rope,  $\Delta_x$  is the length variation of the spring and  $k$  represents the stiffness coefficient of spring.

### III. THE ANALYSIS OF KINEMATIC SPACE AND STATIC LIFTING

In this section, kinematic space and static lifting force analysis of SRL are compared with the human upper limb. For simplification, this emulation is based on the following assumptions: 1) the mass of the structure is ignored due to it is much lower compared to the end load; 2) emulation analysis is performed in a vertical plane which is more valuable than other planes; 3) in parallel mode, the orientation change of the end effector is not concerned, which makes the 3-DOF hexagon mechanism can be simplified to a 2-DOF pentagonal mechanism; 4) the torques of actuators are restricted to no more than 50 N·m. The simplified configuration is shown in Fig. 9. The initial parameters and joints ROM of the parallel

configuration of SRL are listed in Table I. The specifications of the human upper limb and series configuration of SRL are shown in Table II. The specific parameters of the human upper limb were consistent with the biomechanical data of the 50th

percentile of males [17], [18]. In the parallel mode, considering the singular configuration and the uniqueness of the solution, the active joint motion range has a certain limit.

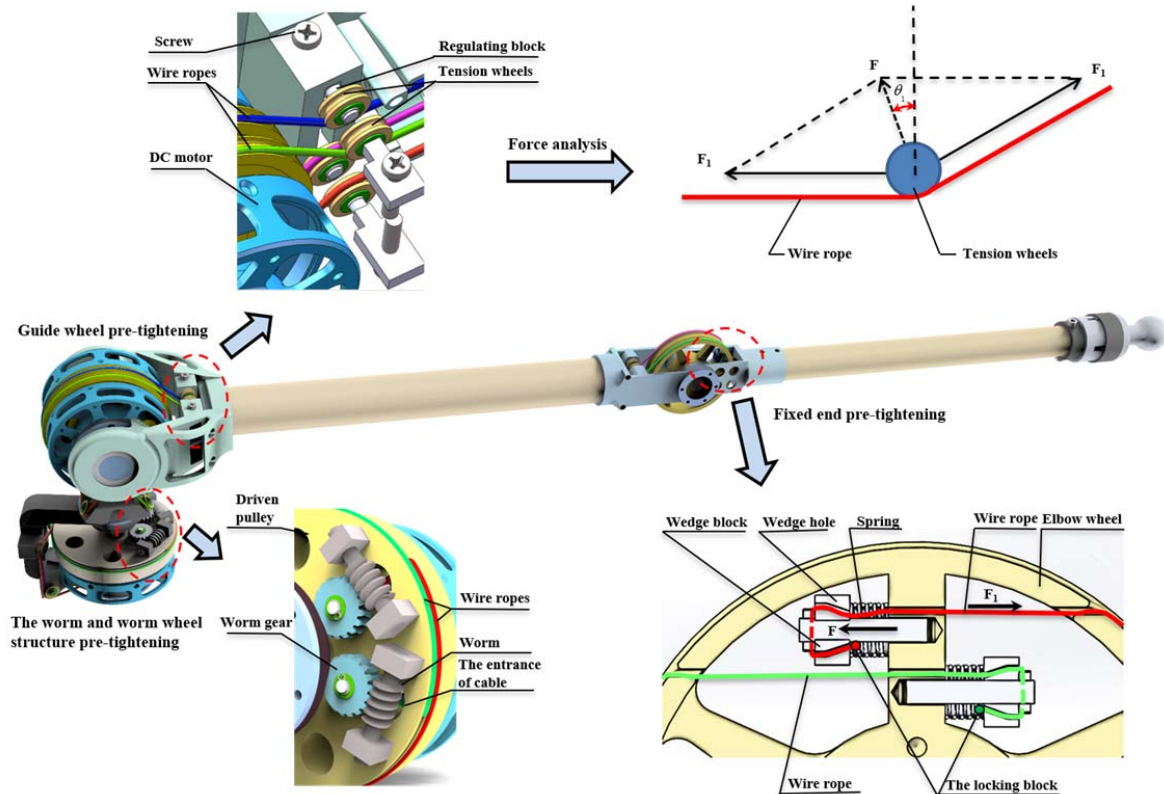


Fig. 8 The arrangement of pre-tensioner

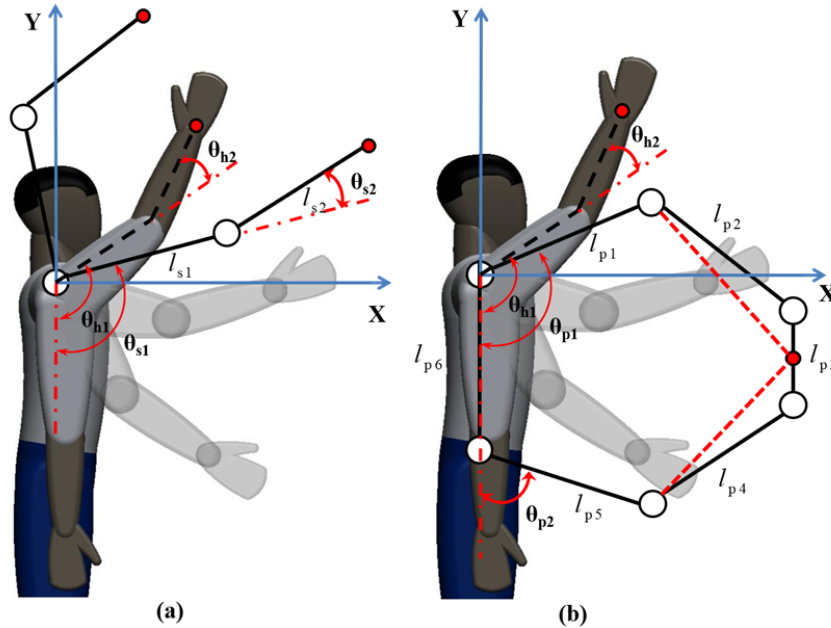


Fig. 9 (a) The simplified configuration of series mode, (b) the simplified configuration of parallel mode

TABLE I  
THE INITIAL PARAMETERS OF THE PARALLEL CONFIGURATION OF SRL

Type	$l_{p1}(l_{p3})$ (mm)	$l_{p2}(l_{p4})$ (mm)	$l_{p3}$ (mm)	$l_{p0}$ (mm)	Movement range of $\theta_{p1}$	Movement range of $\theta_{p2}$
Parallel configuration	350	330	150	300	60°~180°	0°~120°

TABLE II  
THE SPECIFICATIONS OF HUMAN UPPER LIMB AND SERIES CONFIGURATION OF SRL

Type	$l_{h1}/l_{s1}$ (mm)	$l_{h2}/l_{s2}$ (mm)	Movement range of $\theta_{h1}/\theta_{s1}$	Movement range of $\theta_{h2}/\theta_{s2}$
Human upper limb	330	254	15°~135°	0°~140°
Series configuration	350	330	60°~290°	-120°~120°

The motion space is determined by the length of the limb and the ROM of the driving joints. Firstly, the motion space is obtained by inverse kinematics when the distal position is roughly defined, and then the maximum supporting force in motion space is acquired by the following formulation [19]:

$$F_{max} = J^{T-1} \tau_{max}, \quad (12)$$

where  $F_{max}$  is the terminal maximum output force,  $J^T$  is the transpose of the Jacobian matrix and  $\tau_{max}$  represents the maximum output torque given in hypothesis. The simulation results are shown in Fig. 10.

The depth of the color indicates the maximum static output force at the current position. The red boundary represents the ROM of the human upper limbs. By comparing Fig. 10 (a) with (c), it is obvious to notice that both of human upper limb and series structure have a similar output performance that the output force varies with the distance from the X-axis and the maximum force at both far-end of workspace is below 100N. However, the workplace of the series structure is much larger than the human upper limb. By comparing Fig. 10 (a) with (b), the parallel structure performs a better output ability with the maximum force reaching 300N at the edge of the workspace. However, the workplace of parallel structure does not completely that of a human upper limb. In some special areas, due to the dead zone effect, the maximum output force even reaches 500N. Therefore, the design of a variable configuration makes the SRL proposed in this paper is more practical and advantageous.

#### IV. DISCUSSION AND CONCLUSION

In this paper, a reconfigurable SRL based on differential actuated joints is described. As an SRL with variable configurations and the cable-driven transmission, it had the characteristics of high precision, large movement space, and strong carrying capacity. Two kinds of cable-driven mechanical structures based on guide pulleys and differential actuated joints were designed, and two wire rope pre-tightening mechanisms were also designed to improve the reliability and accuracy of cable-driven transmission. To reduce the rotational inertia of the whole limb, all motors were placed near the back. Moreover, the self-designed bearings used in this article greatly simplified the structure and reduced the cost. The proposed SRL also could have a larger workspace and better supporting performance compared to the human limb. Future studies will focus on simplifying the structure, analyzing dynamics and

designing a reasonable control system.

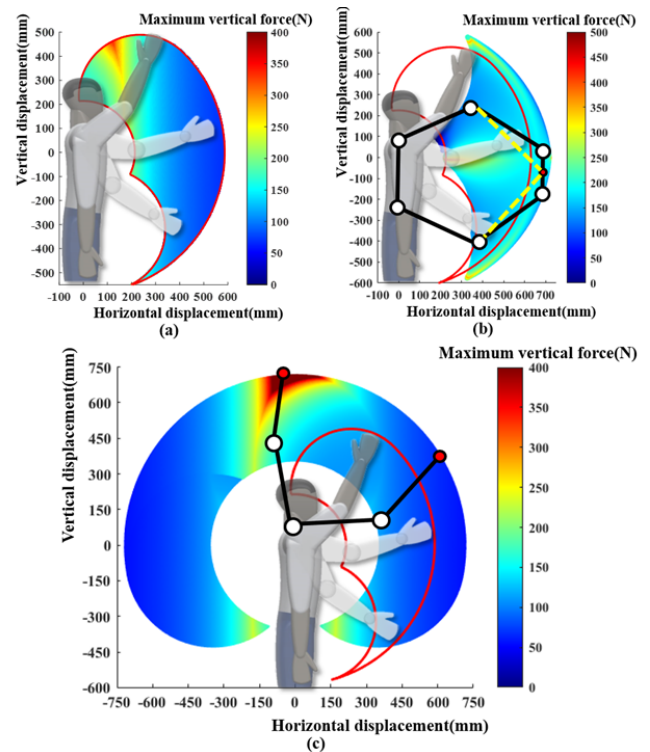


Fig. 10 (a) Static simulation of the human upper limb, (b) static simulation of series structure, (c) static simulation of parallel structure

#### ACKNOWLEDGMENT

The work reported in this paper is supported by The National Key Research and Development Program of China under Grant 2018YFB1305400.

#### REFERENCES

- [1] R. Gopura, D. S. V. Bandara, K. Kiguchi, "Developments in hardware systems of active upper-limb exoskeleton robots: A review," *Robotics and Autonomous Systems*, Vol. 75, pp. 203–220, 2016.
- [2] B. Llorens-Bonilla, F. Parietti, H. H. Asada, "Demonstration-based control of supernumerary robotic limbs," *Intelligent Robots and Systems (IROS)*, pp. 7–12, 2012.
- [3] C. Davenport, F. Parietti, H. H. Asada, "Design and biomechanical analysis of supernumerary robotic limbs" 5th annual dynamic systems and control conference joint with the 11th motion and vibration conference, pp. 787–793, 2012.
- [4] F. Parietti, H. H. Asada, "Supernumerary robotic limbs for aircraft fuselage assembly: body stabilization and guidance by bracing" *IEEE International Conference on Robotics and Automation (ICRA)*, pp. 1176–1183, 2014.
- [5] D. Prattichizzo, M. Malvezzi, I. Hussain, "The sixth-finger: a modular

- extra-finger to enhance human hand capabilities” The 23rd IEEE International Symposium on Robot and Human Interactive Communication, pp. 993-998, 2014.
- [6] F. Y. Wu, H. H. Asada, “Decoupled motion control of wearable robot for rejecting human induced disturbances” IEEE International Conference on Robotics and Automation (ICRA), pp. 1-8, 2018.
- [7] F. Y. Wu, H. H. Asada, ““Hold-and-manipulate” with a single hand being assisted by wearable extra fingers” IEEE International Conference on Robotics and Automation (ICRA), pp. 6205-6212, 2015.
- [8] F. Y. Wu, H. H. Asada, “Implicit and intuitive grasp posture control for wearable robotic fingers: A data-driven method using partial least squares”. IEEE Transactions on Robotics, Vol. 32, pp. 176–186, 2016.
- [9] Y. Hu, S. Leigh, P. Maes, “Hand development kit: Soft robotic fingers as prosthetic augmentation of the hand” Adjunct Publication of the 30th Annual ACM Symposium on User Interface Software and Technology, pp. 27-29, 2017.
- [10] B. L. Bonilla, H. H. Asada, “A robot on the shoulder: Coordinated human-wearable robot control using coloured petri nets and partial least squares predictions” IEEE International Conference on Robotics and Automation (ICRA), pp. 119-125, 2015.
- [11] F. Parietti, H. H. Asada, “Dynamic analysis and state estimation for wearable robotic limbs subject to human-induced disturbances” IEEE International Conference on Robotics and Automation, pp. 3880-3887, 2013.
- [12] V. Vatsal, G. Hoffman, “Design and Analysis of a Wearable Robotic Forearm” IEEE International Conference on Robotics and Automation (ICRA), pp. 1-8, 2018.
- [13] P. H. Nguyen, C. Sparks, S. G. Nuthi, “Soft poly-limbs: Toward a new paradigm of mobile manipulation for daily living tasks” Soft robotics, Vol. 6, pp. 38–53, 2019.
- [14] Y. F. Lu, D. P. Fan, D. J. Sheng, “Design consideration for precise cable drive” Advanced Materials Research, Vol. 305, pp. 37–41, 2011.
- [15] Y. Chen, G Li, Y Zhu, “Design of a 6-DOF upper limb rehabilitation exoskeleton with parallel actuated joints” Bio-medical materials and engineering, Vol. 24, pp. 2527–2535, 2014.
- [16] W. Wang, “Machine design handbook (New edition)” China Machine Press, Beijing, China, 2004, Vol. 3, pp. 211–266.
- [17] A. R. Tilley, “The measure of man and woman: human factors in design” John Wiley & Sons, 2001.
- [18] M. H. Rahman, M. Saad, J. P. Kenné, “Modeling and control of a 7DOF exoskeleton robot for arm movements” IEEE International Conference on Robotics and Biomimetics (ROBIO), pp. 245-250, 2009.
- [19] J. J. Craig, Introduction to robotics: mechanics and control, Pearson Education India, 2009, pp. 148–159.